CPT: Pharmacometrics & Systems Pharmacology

ARTICLE OPEN ACCESS

A Population Pharmacokinetic Model to Inform Extension of the Eteplirsen Dosing Regimen Across the Broad DMD Population

Yogesh Patel | Larry Orogun | Nicole Yocum | Louise R. Rodino-Klapac | Lilly East

Sarepta Therapeutics, Inc., Cambridge, Massachusetts, USA

Correspondence: Yogesh Patel (ypatel@sarepta.com)

Received: 16 September 2024 | **Revised:** 30 January 2025 | **Accepted:** 3 February 2025

Funding: This work was funded by Sarepta Therapeutics Inc.

Keywords: dose | pediatric | pharmacokinetics | population

ABSTRACT

Duchenne muscular dystrophy (DMD) is characterized by progressive, irreversible muscle damage that usually leads to premature death from cardiac or respiratory failure. Eteplirsen is a phosphorodiamidate morpholino oligomer and the first antisense oligonucleotide (ASO) approved for the treatment of patients with exon 51 skip-amenable DMD. This analysis presents the first population pharmacokinetics (PK) modeling and simulation performed for the ASO drug class in DMD. Study objectives were to characterize the population PK of eteplirsen in patients with DMD across a broad age range and to identify the impact of covariates on eteplirsen exposure to guide clinical dosing. Plasma concentration data were pooled from six clinical studies of male patients with DMD across the age range of 6 months to 4 years (1 study) and 4–16 years (5 studies). Doses ranged from 0.5 to 50 mg/kg/week across different studies. A three-compartment model with a linear elimination described the eteplirsen plasma concentration data well. Body weight effect on all PK parameters and eGFR, and age (≤4 years vs. >4 years) effect on systemic clearance were key determinants of variability in the final model. Simulations showed similar exposures for eteplirsen (30 mg/kg intravenously once weekly) across different age groups (0.5 to <2, 2 to <4, 4 to <7, and 7 to ≤16 years). These findings support the existing eteplirsen dosing paradigm of uniform weight-based dosing at 30 mg/kg/week across the broad age range of the target DMD population (6 months to adolescence).

1 | Introduction

Duchenne muscular dystrophy (DMD) is an X-linked muscle-wasting disease that affects approximately 1 in 3500–5000 live male births [1–5]. DMD is caused by mutations in the *DMD* gene that encodes the dystrophin protein [6, 7]. In patients with DMD, progressive and irreversible muscle damage is ongoing at birth due to the lack of functional dystrophin, leading to ambulatory difficulties, cardiomyopathy, the need for assisted ventilation, and premature death [6–8]. Motor function development in patients aged ≤7 years often masks muscle degeneration, which may lead to delayed diagnosis, whereas patients aged >7 years tend to exhibit progressive muscle deterioration and consequently declining ambulatory function [9–12].

In previous decades, patients with DMD died in their teenage years; however, advances in management, a greater understanding of disease pathology, and the emergence of novel therapeutics have extended the lifespan of patients into their 30s [13]. Treatment for DMD is focused on managing disease symptoms with physiotherapy, corticosteroids, cardiac medications, and ventilation support; however, several targeted therapeutic approaches are now available [6, 7]. Initiating treatment early, before significant muscle degeneration has

Larry Orogun was affiliated with Sarepta at the time of this analysis.

Summary

- What is the current knowledge on the topic?
  - Eteplirsen is an exon 51-skipping phosphorodiamidate morpholino oligomer (PMO).
  - Clinical studies have shown that eteplirsen is well tolerated and demonstrate dystrophin production in patients aged ≥7 years with Duchenne muscular dystrophy (DMD) with mutations amenable to exon 51 skipping.
- What question did this study address?
  - This study characterized a population pharmacokinetics (PK) model of eteplirsen in patients with DMD across a broad age range to identify the impact of covariates on eteplirsen exposure to guide clinical dosing.
- What does this study add to our knowledge?
  - This analysis presents the first population PK modeling and simulation performed for the antisense oligonucleotide (ASO) drug class in DMD.
  - The results support consistency of eteplirsen exposure across a broad age range using a weight-based dosing regimen and extrapolation of the uniform 30 mg/kg/week dosing regimen to younger patients.
- How might this change drug discovery, development, and/or therapeutics?
  - This study demonstrates the application of population PK modeling to characterize a PMO; this method can be extended to other PMOs and ASOs for the treatment of DMD and other rare diseases.

occurred, may improve clinical outcomes [12, 14–16]. Targeted exon skipping within the *DMD* gene can be an effective treatment approach for DMD [17, 18]. Phosphorodiamidate morpholino oligomers (PMOs) are exon-skipping therapies that demonstrate strong sequence-specific binding to ribonucleic acid (RNA) targets, which alters pre-RNA splicing to restore the reading frame and allow the production of an internally shortened but functional dystrophin protein [17, 19, 20]. Eteplirsen is a PMO approved by the United States (US) Food and Drug Administration (FDA) for patients with DMD who have a confirmed genetic mutation that is amenable to exon 51 skipping [21].

Both preclinical and clinical evaluations of PMOs have demonstrated favorable, consistent, and predictable safety profiles [18, 22–28]. Data from the first clinical trial of eteplirsen in boys with DMD aged 6–48 months also support the safety and tolerability of eteplirsen at the approved 30 mg/kg dose in this younger population [29]. Clinical studies of eteplirsen 30 or 50 mg/kg weekly in patients aged >4 years indicate that eteplirsen is well tolerated and demonstrate dystrophin production [18, 30]. Studies have also shown that eteplirsen attenuates pulmonary and ambulatory decline and prolongs survival compared with mutation-matched natural history cohorts [31, 32].

The pharmacokinetic (PK) characteristics for eteplirsen at doses ranging from 0.5 to 30.0 mg/kg have been described previously in different age groups, using serial and sparse sampling for the older and younger patients, respectively. Findings demonstrate eteplirsen to have a short half-life and rapid renal clearance [29, 33].

The objective of this analysis was to characterize the population PK characteristics of eteplirsen across a broad range of patients with DMD, from pediatric to adolescent patients, to further support comparable PK characteristics across the broad DMD population. Pooled data obtained from completed clinical studies were analyzed. Additionally, the population PK model was used to identify the impact of covariates on eteplirsen exposure to guide clinical dosing.

2 | Methods

2.1 | Study Design and Patient Population

Plasma concentration data from six completed eteplirsen clinical studies that enrolled patients with DMD, ranging in age from 6 months to 16 years and with mutations amenable to exon 51 skipping, were pooled for this population PK analysis (Table 1). As reported previously, all studies were conducted in accordance with the appropriate ethical standards and institutional review board requirements, and informed consent was obtained from all participants [29–31, 33].

2.2 | PK Sampling

Patients were included in this pooled analysis if they had received at least one dose of eteplirsen and had at least one evaluable PK sample (defined as a sample where the concentration was quantifiable and the time of observation, time of dose, and dose amount were available or reliably assumed). Plasma samples (extensive or sparse) were collected post dosing following weekly approximate 1-h intravenous (IV) infusions of eteplirsen. PK sampling times for each study are detailed in Method S1. PK data included in this analysis were eteplirsen plasma concentration measurements and associated observation times. Concentrations with missing observation or dosing times that could not be imputed based on nominal times were excluded.

2.3 | Covariates

Covariates of interest and physiological parameters known to show a meaningful effect on the PK parameters were selected for evaluation in the population PK analysis and included body size (total body weight, lean body mass, body mass index [BMI], body surface area), baseline ambulatory status, demographics (age, race, ethnicity, genotype), concomitant medications (steroid strength, single or multiple steroids), renal function (indicated by estimated glomerular filtration rate [eGFR]), renal biomarkers if available (e.g., cystatin C or kidney injury molecule 1), and liver function (alanine aminotransferase, aspartate aminotransferase, bilirubin, albumin). Potential covariates for which there was no scientific rationale were not assessed.

Because creatinine is a byproduct of the muscle breakdown occurring in patients with DMD, creatinine clearance was not an

TABLE 1 | Eteplirsen clinical study and patient characteristics.

	NCT03218995 (study 4658-102) [29]	NCT01396239 (study 4658-201) [18]	NCT01540409 (study 4658-202) [18]	NCT02420379 (study 4658-203) [34]	NCT00844597 (study 4658-28) [33]	NCT02255552 (study 4658-301) [30]	All studies
Clinical study characteristics							
Study type	Phase II, multicenter, open-label, dose-escalation	Phase II, randomized, double-blind, placebo-controlled	Phase II, open-label, multiple-dose extension study of 4658-US-201	Phase II, open-label, multicenter study	Phase I/II, open-label, dose-escalation	Phase III, multicenter, open-label, non-randomized	—
Eteplirsen dose	2, 4, 10, 20, then 30 mg/kg weekly for up to 96 weeks	30 mg/kg or 50 mg/kg weekly for 24 weeks	30 mg/kg or 50 mg/kg weekly for up to an additional 284 weeks	30 mg/kg weekly for 96 weeks	0.5, 1.0, 2.0, 4.0, 10.0, and 20.0 mg/kg weekly for 12 weeks	30 mg/kg weekly for 96 weeks	—
Eligible patient age	6–48 months	7–13 years	7–13 years	4–6 years	5–15 years	7–16 years	—
Patient characteristics							
No. of treated patients	15	12	12	26	17	75	157
Median (range) age, years	2.34 (0.55–4.07)	9.76 (7.37–11.0)	10.3 (7.91–11.6)	5.29 (4.09–7.08)	9.52 (6.05–13.3)	9.09 (7.14–16.4)	8.37 (0.55–16.4)
Median (range) weight, kg	13.3 (6.80–19.8)	34.6 (23.2–42.0)	35.4 (23.9–48.1)	18.8 (14.3–36.2)	30.3 (21.2–62.0)	32.3 (20.2–68.9)	27.1 (6.80–68.9)
Median (range) eGFR, mL/min/1.73 m^2	142 (115–161)	137 (127–163)	138 (130–156)	149 (105–180)	145 (141–145)	143 (85.5–174)	145 (85.5–180)

Abbreviations: eGFR, estimated glomerular filtration rate; PK, pharmacokinetic.

appropriate marker of renal function for this analysis. Instead, continuous serum cystatin C was used to estimate the eGFR using the CKD-EPI equation [35]. The CKD-EPI equation was selected to calculate eGFR because published studies have established cystatin C as the preferred biomarker for monitoring renal function in DMD [36–38].

If > 10% of any covariate value was missing, that covariate was not included in the analysis; otherwise, missing covariates were imputed using a single imputation method, based on the remaining available data. eGFR was not measured in Study 4658-28 and was imputed using the median eGFR observed in patients of the same age.

2.4 | Exploratory Data Analysis

Prior to model development, exploratory data analysis involved generation of graphical and tabular summaries of covariates and measures of exposure to identify missing data and outliers. These included summary statistics of baseline covariates (overall and stratified by study), correlation plots between continuous covariates, box and whisker plots between continuous and categorical covariates (overall and stratified by study), and plots of eteplirsen concentration and eteplirsen dose-normalized concentration over time.

2.5 | Base Model Development

A number of exponential phases observed in the PK profile during the exploratory data analysis guided the selection of the base model for the evaluation. The initial model was a two-compartment model characterized by clearance (CL) after IV dosing, central volume of distribution (V_1), intercompartmental clearance for peripheral compartment (Q), and volume of distribution in peripheral compartment (V_2), with appropriate random effect distributions. A three-compartment model characterized by CL, V_1, intercompartmental clearance for peripheral compartments 1 and 2 (Q_2 and Q_3), and volume of distribution in peripheral compartments 1 and 2 (V_2 and V_3) was also evaluated. Assessment of model adequacy and decisions about increasing or decreasing model complexity were driven by the data and guided by goodness-of-fit criteria (visual inspection of diagnostic plots, favorable convergence of the minimization routine, credibility and accuracy of parameter estimates, correlation between model parameter estimates [< 0.95], and Akaike information criterion).

Effect of body size on the PK parameters was evaluated using different models, including fixed and estimated allometric scaling using body weight across the age range and fixed allometric exponents by age [39] and using power model with the other body size parameters (e.g., BMI, body surface area, lean body mass).

2.5.1 | Interindividual Random Effects and Residual Error Specifications

Nonlinear mixed effects models were developed to evaluate covariate effect on PK parameters and describe the eteplirsen PK data. Model parameters were modeled in the log-domain. All interindividual error terms were described by an additive model in the log-domain

$$\hat{P} = \mathrm{LN}(\theta)$$

$$P_i = e^{\left(\hat{P}+\eta_{P_i}\right)}$$

where θ is the estimated model parameter, $\hat{P}$ is the log-transformed typical population value of the parameter, P_i is the estimated individual parameter value for individual i, η_{P_i} are individual-specific interindividual random effects for individual i and parameter P and are assumed to be normally distributed with mean zero and standard deviation ω ($\eta_i \sim N\left(0, \omega^2\right)$). Interindividual variability (% coefficient of variation [%CV]) was calculated as

$$\%\,\mathrm{CV} = 100 \cdot \sqrt{\left(e^{\omega^2} - 1\right)}$$

Plasma concentrations were log-transformed for model-fitting purposes and back-transformed to normal scale for diagnostic plots. The residual error model was described by an additive error model on the log domain

$$\log\left(C_{ij}\right) = \log\left(\hat{C}_{ij}\right) + \varepsilon_{ij}$$

where C_{ij} is the jth measured observation in individual i, $\hat{C}_{ij}$ is the jth model predicted value in individual i, and ε_{ij} is the additive residual random error for individual i and measurement j and is assumed to be identically distributed with mean zero and standard deviation σ ($\varepsilon_{ij} \sim NID\left(0, \sigma^2\right)$).

2.6 | Covariate Analysis

A covariate modeling approach emphasizing parameter estimation while characterizing relevant covariate effects was implemented. A full model was constructed with care to avoid correlation or collinearity in predictors (covariates with correlation coefficients > 0.6 were not simultaneously included as potential predictors). Population parameters, including fixed effects parameters (covariate coefficients and structural model parameters) and random effects parameters, were estimated. An exploratory assessment of any remaining trends was conducted by graphical inspection of all covariate effects. Inferences about the relevance of parameters were based on the resulting parameter estimates of the full model and measures of estimation precision (asymptotic standard errors). No hypothesis testing was conducted.

2.7 | Final Model Evaluation

The precision of the parameters was derived using the standard errors of the estimates provided from the MCMC Bayesian analysis in the accumulation phase of the NONMEM run. Longitudinal visual predictive checks (VPCs) were performed by generating 500 Monte Carlo simulation replicates of the analysis dataset using the final population PK models, plotting observed

eteplirsen plasma concentration data, and overlaying the data with the corresponding simulated median, 5th, and 95th percentiles. A VPC for Study 4658–102 was performed using the same method to evaluate PK in younger patients aged 6–48 months. The final model was also evaluated using other methods including goodness-of-fit plots, model-derived exposure parameters, and forest plots.

Significance of covariate effects was evaluated using forest plots where eteplirsen PK exposures (e.g., area under the concentration–time curve for a dosing interval at steady state [AUC_{ss}] and maximum concentration in the dosing interval [C_{max}] for a reference dose) relative to typical subject over a relevant covariate range were plotted against the reference range. The parameter estimate and 95% CI for PK exposures were computed using uncertainty in the final parameter estimates. The reference range of 0.8–1.67 for PK exposure relative to typical subject was used to further evaluate the significance and impact of the covariate effects. In the absence of defined exposure boundaries for a minimally efficacious dose to a maximally tolerated dose, conservative estimates were used instead, based on existing clinical safety and efficacy data. An upper bound of 1.67 was selected based on the demonstrated clinical safety at 50 mg/kg relative to therapeutic dose of 30 mg/kg in DMD patients. A lower bound of 0.8 was an empirical estimate based on an assumed 25% bioequivalence criteria.

2.8 | Simulation of Eteplirsen Plasma Exposures

Stochastic simulations were performed to predict eteplirsen plasma exposures (AUC_{ss} and C_{max} at steady state [$C_{max,ss}$]) in pediatric patients aged 6 months to 16 years. A virtual population for stochastic simulation was generated based on weight distribution by age provided in CDC NHANES database for patients aged < 2 years [40], West et al. for patients aged 2–12 years [41], and analysis dataset for patients aged > 12 years. The simulated population included 16,000 individuals receiving weekly dosing of eteplirsen 30 mg/kg via 1-h IV infusion. Patients were assumed to be at steady state when the first dose was administered, considering the relatively short elimination half-life and weekly dosing frequency, and were followed 24 h post dose (0.1-h increments). Simulations were performed using the final model, including interindividual variability and parameter uncertainty.

2.9 | Computational Software

Data manipulation, visualization, and simulations were conducted using R version 3.5.1. All analyses were conducted via nonlinear mixed effects modeling using NONMEM version 7.4 (ICON Development Solutions, Hanover, MD, USA).

3 | Results

3.1 | Analysis Datasets and Patient Characteristics

The population PK dataset used in this analysis contained 3258 quantifiable eteplirsen observations from 157 patients; this dataset excluded 37 (1.1%) samples that were below the limit of quantification. The median age was 8.4 years (range: 6 months to 16.4 years), the median weight was 27.1 kg (range: 6.8–68.9 kg), and the median eGFR was 145 mL/min/1.73 m^2 (range: 85.5–180 mL/min/1.73 m^2) (Table 1). Summary of additional patient characteristics is provided in Table S1. Scatter plots for the correlation between continuous covariates are presented in Figure S1. All patients were assigned a single dose of eteplirsen for the duration of each study (0.5, 1.0, 2.0, 4.0, 10.0, or 20.0 mg/kg in 4658–28; 30 or 50 mg/kg in 4658-US-201 and 4658-US-202; 30 mg/kg in 4658-203 and 4658-301), except those in the dose-escalation study (4658-102; escalation from 2 mg/kg to 4, 10, 20, and then 30 mg/kg).

3.2 | Exploratory Data Analysis

Concentration–time plots showed that eteplirsen concentration generally peaked immediately following the end of infusion, followed by rapid distribution phase for the next 2–3 h, and then steady elimination phase over the course of 1 day. The dose-normalized eteplirsen concentration versus time-after-dose profiles across the different dose groups were superimposed without evidence of any clear trends. Therefore, PK was assumed to be linear across the dose range investigated (0.5–50 mg/kg; Figure 1). Considering the pediatric population, age and body weight were highly correlated with a correlation coefficient of 0.781 (Figure S1), which precluded estimation of effects of both covariates, body weight and age, on CL simultaneously. As expected, eGFR (mL/min/1.73 m^2) showed a poor correlation with age and body weight.

3.3 | Base Model

A two-compartment model was unable to characterize the eteplirsen elimination, whereas a three-compartment population PK model with zero-order absorption and first-order elimination from the central compartment and IIV on all PK parameters except on V_3 and Q_3 provided optimal fit to the observed plasma PK data and was selected as the final base model. The model was parameterized in terms of CL, V_1, V_2, V_3, Q_2, and Q_3. Random effects were included to estimate the interindividual variability and the residual variability of the data. Model development was initially planned to use the first-order conditional estimation method with η-ε interaction (FOCEI) for all population PK model runs. However, models were frequently unable to converge using the FOCEI method. Population and individual model parameters were therefore estimated using the importance sampling assisted by mode a posteriori method. The body weight effects on volume and clearance parameters using fixed allometric exponents of 0.75 for clearance parameters and 1 for volume parameters described data well and were included in the base model. Alternative models to characterize body size effect on the model parameters resulted in non-identifiability, unreasonable estimates in some of the parameters, higher objective function values, higher model condition number, increased residual error, and/or poor model diagnostics.

Interindividual random effect distributions were modeled using an additive model on log domain on CL, V_1, V_2, and Q_2, with covariance terms between all effects. Residual random effects

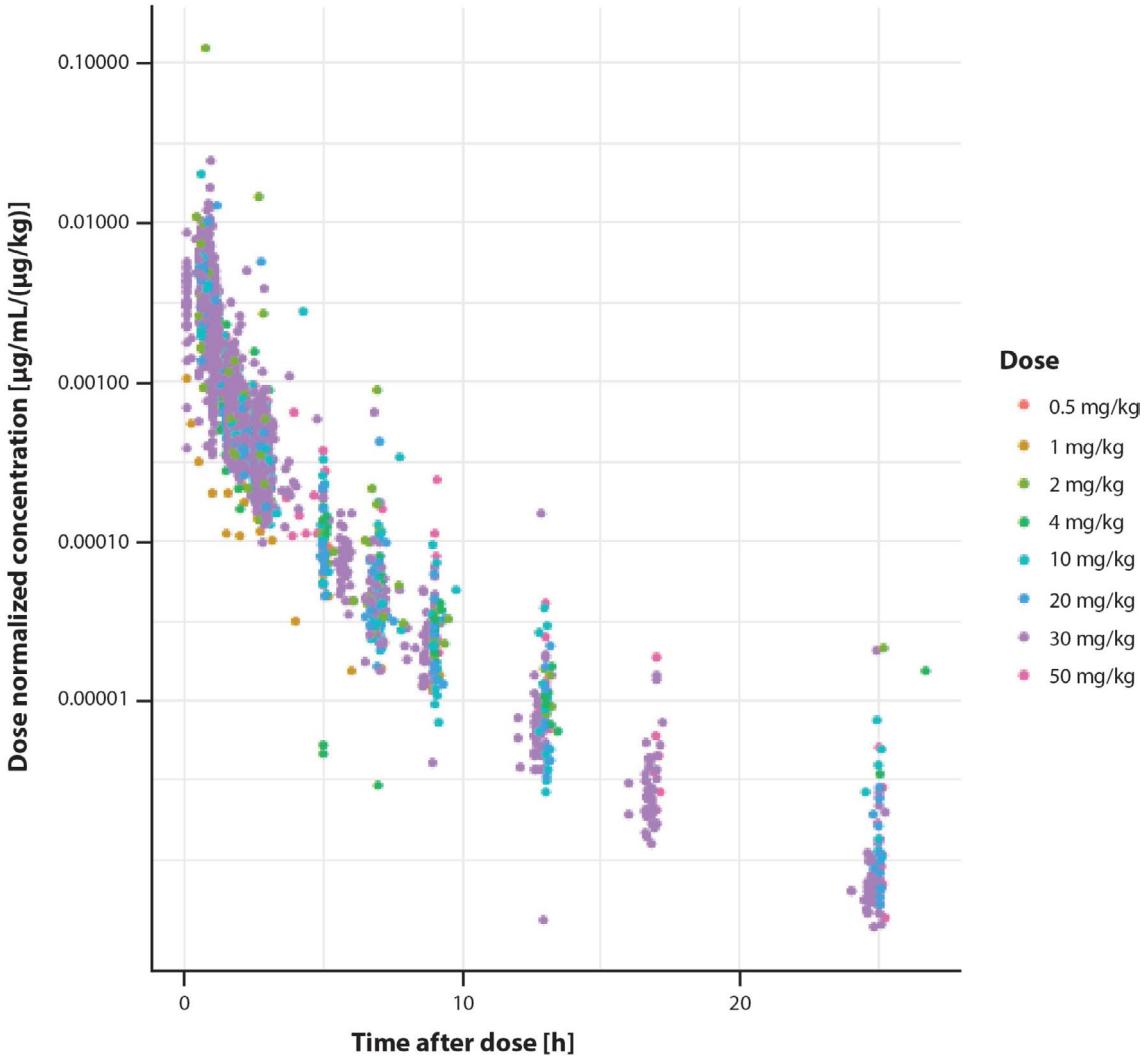

FIGURE 1 | Dose-normalized eteplirsen concentration–time data plotted on a log scale, colored by different dose groups.

were described with an additive error model in the log domain. Overall, fixed effect and random variability parameters were precisely estimated in the base model (% relative standard error (RSE) of ≤9.56% for fixed effect parameters and ≤10.4% for random effect parameters).

3.4 | Final Model

The final model was developed starting from the base model using a full covariate model approach emphasizing parameter estimation while assessing relevant covariate effects. During covariate evaluation, eGFR and age were identified as important covariates on CL to include in the final model. The parameter estimates for the final population PK model are shown in Table 2, and the relationship between parameter and covariate effect is presented in Equations (1–6).

$$\mathrm{CL}_i = \exp\left(\left[\mathrm{ifelse}(\mathrm{Age}_i > 4\mathrm{yrs}, \theta_1, \theta_2)\right] + \eta_{1i}\right) \times \left(\frac{\mathrm{WT}_i\mathrm{kg}}{37\ \mathrm{kg}}\right)^{0.75} \times \left(\frac{\mathrm{eGFR}_i}{145}\right)^{\theta s} \quad (1)$$

$$V_1 i = \exp\left(\theta_3 + \eta_{2i}\right) \times \left(\frac{\mathrm{WT}_i\mathrm{kg}}{37\ \mathrm{kg}}\right)^{1} \quad (2)$$

$$V_2 i = \exp\left(\theta_4 + \eta_{3i}\right) \times \left(\frac{\mathrm{WT}_i\mathrm{kg}}{37\ \mathrm{kg}}\right)^{1} \quad (3)$$

$$Q_2 i = \exp\left(\theta_5 + \eta_{4i}\right) \times \left(\frac{\mathrm{WT}_i\mathrm{kg}}{37\ \mathrm{kg}}\right)^{0.75} \quad (4)$$

$$V_3 i = \exp\left(\theta_6\right) \times \left(\frac{\mathrm{WT}_i\mathrm{kg}}{37\ \mathrm{kg}}\right)^{1} \quad (5)$$

$$Q_3 i = \exp\left(\theta_7\right) \times \left(\frac{\mathrm{WT}_i\mathrm{kg}}{37\ \mathrm{kg}}\right)^{0.75} \quad (6)$$

Value WT_i is individual body weight. Parameters θ_1, θ_3, θ_4, θ_5, θ_6, and θ_7 are the population mean estimates of the reference subject for CL_i, V_{1i}, V_{2i}, Q_{2i}, V_{3i}, and Q_{3i}, respectively. Parameter

TABLE 2 | Population PK parameters in the final model.

Parameter	Description	Units	Estimate	95% CI
θ_1	CL_{older}	L/h	6.98	6.68–7.31
θ_2	$CL_{younger}$	L/h	4.97	4.48–5.47
θ_3	V_1	L	2.21	1.93–2.55
θ_4	V_2	L	2.23	1.90–2.64
θ_5	Q_2	L/h	0.334	0.262–0.422
θ_6	V_3	L	4.12	3.81–4.43
θ_7	Q_3	L/h	3.49	3.29–3.70
θ_8	eGFR on CL	—	1.60	1.33–1.92
ω_{CL}	IIV in CL	CV%	23.5	20.2–27.4
ω_{CL-V_1}	Cov(CL, V_1)	—	0.0541	0.0264–0.0924
ω_{CL-V_2}	Cov(CL, V_2)	—	0.110	0.0719–0.159
ω_{CL-Q_2}	Cov(CL, Q_2)	—	0.167	0.116–0.234
ω_{V_1}	IIV in V_1	CV%	49.8	40.1–61.7
$\omega_{V_1-V_2}$	Cov(V_1, V_2)	—	0.193	0.103–0.315
$\omega_{V_1-Q_2}$	Cov(V_1–Q_2)	—	0.295	0.178–0.447
ω_{V_2}	IIV in V_2	CV%	70.5	55.6–91.5
$\omega_{V_2-Q_2}$	Cov(V_2, Q_2)	—	0.470	0.310–0.695
ω_{Q_2}	IIV in Q_2	CV%	103	79.8–137
σ_{RV}	RV	CV%	35.1	34.1–36.1

Note: Eta-shrinkage for CL, V_1, V_2, and Q_2 was 11.0%, 22.1%, 24.9%, and 20.4%, respectively. Epsilon-shrinkage for the residual variability was 67.7%. The 95% CI is for the parameter estimate. Estimates of 95% CI were generated by determining the 2.5th and 97.5th quantiles of the posterior parameter estimates in the accumulation phase.
Abbreviations: CI, confidence interval; Cov, covariance; CV%, coefficient of variation; IIV, interindividual variability; PK, pharmacokinetic; Q_2, intercompartmental clearance for peripheral compartment 1; RV, residual variability; V_1, central volume of distribution; V_2, volume of distribution in peripheral compartment 1; V_3, volume of distribution in peripheral compartment 2.

θ_2 is the population mean estimate for CL_i in DMD patients with age ≤4 years. Values η_{1i}, η_{2i}, η_{3i}, and η_{4i} (Equations 1–4) are the estimates of IIV in CL_i, V_{1i}, V_{2i}, and Q_{2i}, respectively, for individual *i*. The typical values (95% CI) of CL for the reference patient was 6.98 L/h (6.68–7.31). Body weight was included as a covariate using an allometric function with a fixed exponent of 1 for volume parameters or 0.75 for clearance parameters. A body weight of 37 kg was selected as a reference male DMD patient (>4 years of age) with an eGFR of 145 mL/min/1.73 m^2 to normalize the younger pediatric population (≤4 years old) to an older reference population where the majority of PK data were collected from.

The final model included fixed effects of body weight on all clearance and volume terms, as well as the effects of age and renal function (eGFR) on CL to account for maturation across the age groups and the primary elimination mechanism for eteplirsen (renal excretion). No specific trends observed in the plots of interindividual random effect versus demographic, body size, and laboratory parameter were observed in the final model, which suggested that no additional covariate effects remained to account for in the model (Figures S2 and S3). The eGFR was an important determinant for variability in CL. An increase of approximately 10% in eGFR (to 160 mL/min/1.73 m^2) will increase CL by 14.5% (relative to the estimate of 6.98 L/h in a typical patient), while decreasing eGFR by approximately 10% (to 130 mL/min/1.73 m^2) will decrease CL by 18.4%. The effect of age on CL was evaluated using continuous power model and categorical model. Since body weight and age were highly correlated in the pediatric population, inclusion of a continuous covariate effect of age in addition to body weight resulted in poor characterization of covariate effects. Among the models with categorical covariate effects of age on CL using different age cut-offs, the model with an age cut-off (≤3 years vs. >3 years) was not well estimated considering not enough subjects in the analysis dataset with age ≤3 years (approximately 5.7% of population). The model with an age cut-off (≤4 years vs. >4 years) described the data well and was selected in the final model. Although a slight residual trend in the final model remained in the younger patients (approximately ≤3 years old) (Figure S2), the overall interindividual random effect in these younger subjects is within the variability observed for the rest of the population.

Interindividual variability (%CV) was 23.5% for CL, 49.8% for V_1, 70.5% for V_2, and 103% for Q_2. Residual variability was 35.1% CV using an additive error model in the log domain. Fixed and random effect parameters in the final model were well estimated, based on the width of the 95% CIs.

The final model provided a good description of the data. Goodness-of-fit plots showed good correlation between observed concentrations versus population and individual predicted concentrations of eteplirsen (Figure 2a). Conditional weighted residuals and normalized prediction distribution errors were randomly distributed around zero without specific trends across the range of time and population predicted concentration (Figures 2b, S4, and S5). A prediction-corrected VPC showed that median, 5th percentile, and 95th percentile profiles of observed data were well captured within the 95% CI of the respective profiles of predicted data, which further supported that the final model described the data and variability well (Figures 3a and S6). Further VPC using the final model adequately captured the observed concentration–time profiles in younger patients aged 6–48 months (Study 4658-102), with the majority of observed values lying within the 5%–95% prediction interval in both age cohorts for the study (6–24 months and 24–48 months) (Figure 3b).

3.5 | Significance of Covariate Effects

Body weight, age, and eGFR were found to be key determinants of variability in the PK parameters of AUC_{ss} and $C_{max,ss}$. However, body weight was the only significant covariate, with significance defined as the point estimate and 95% CIs for both lower and upper body weight outside the reference range for both parameters (Figure 4). Neither the impact of a lower

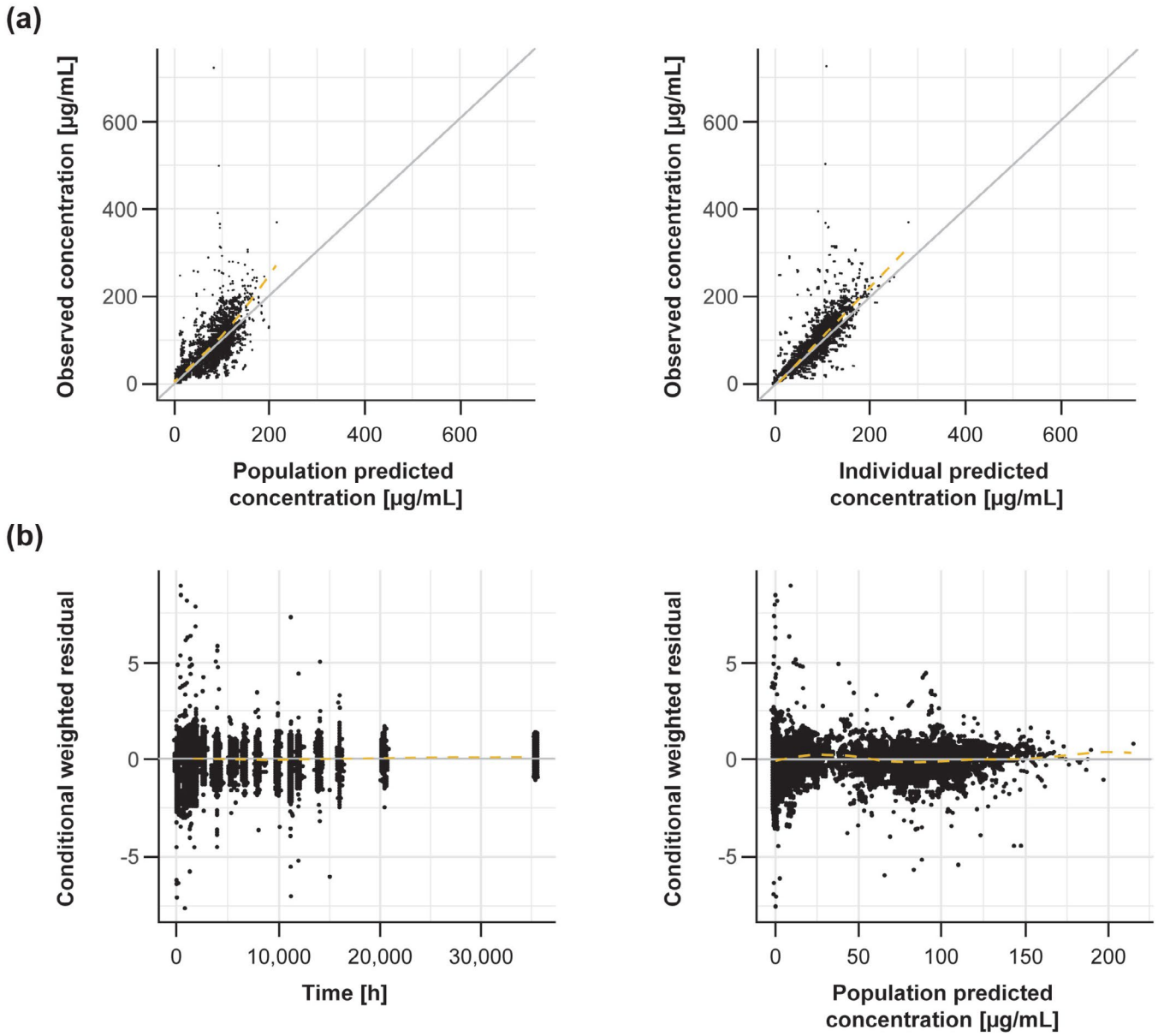

FIGURE 2 | Goodness-of-fit plots. (a) Observed versus population (left) and individual (right) predicted eteplirsen concentration. Observed values are indicated by black circles. The line of identity (solid gray) is included as a reference (X = Y). The dashed yellow line represents a locally weighted scatterplot smoothing (LOESS) line through the data. (b) Conditional weighted residual versus time (left) and population predicted concentration (right). Solid back circles represent individual residual values associated with each observation record. The solid horizontal gray line (residual = 0) is included for reference. The dashed yellow line represents LOESS line through the data.

eGFR nor age ≤ 4 years was statistically significant according to the reference range. The impact of a higher eGFR was inconclusive, as the point estimate was not fully contained within the reference range (Figure 4). Although inconclusive, eGFR was retained in the model based on analysis of model diagnostics and due to renal clearance being the primary elimination mechanism for eteplirsen. The impact of age ≤ 4 years was statistically non-significant on CL as the point estimate and 95% CI for the exposure parameters were within reference range. However, considering the model application for dose extrapolation to younger subjects, the effect of age was considered clinically important and conservative to appropriately capture relatively higher exposures observed in younger subjects compared to older subjects (Figure 4). Since the understanding on the impact of growth/maturation on PMO PK in younger subjects is limited, it is deeed important to include age effect on CL to describe observed difference in addition to the body weight effect informed by the data and the eGFR effect based on the known physiological change in pediatric population and PMO PK.

3.6 | Stochastic Simulations

Exposure was similar across the entire age range (6 months to adolescence), with exposure in younger age groups (0.5 to < 2, 2 to < 4, and 4 to < 7 years) within the range of that seen in older children aged 7 to ≤ 16 years (Figure 5 and Table S2).

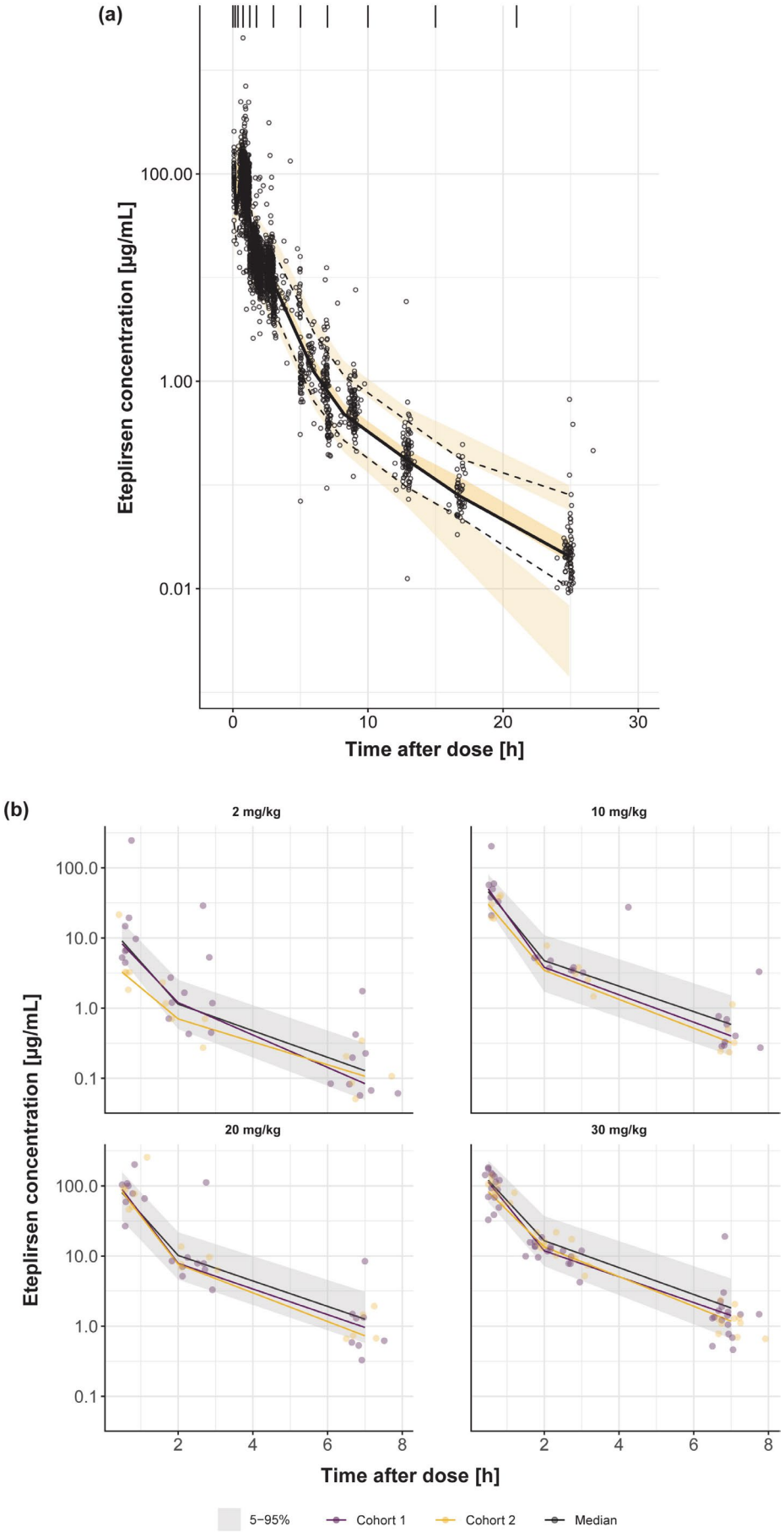

FIGURE 3 | Legend on next page.

FIGURE 3 | Model evaluation. (a) Prediction-corrected visual predicted check of eteplirsen concentration versus time after dose. Black lines represent the median, 5th percentile, and 95th percentile profiles of the observed data. Yellow shaded regions represent the 95% confidence interval of the median, 5th percentile, and 95th percentile profiles of the predicted data. (b) Eteplirsen concentration versus time after dose. Cohort 1 included observations in children aged 24–48 months (purple circles), and cohort 2 included observations in children aged 6–24 months (yellow circles). The solid black, purple, and yellow lines represent the median predicted population, cohort 1, and cohort 2 eteplirsen concentration, respectively. The gray bar is the 5%–95% prediction interval. Timepoints observed were prior to end of infusion, 1–3 h post infusion, and 6–8 h post infusion.

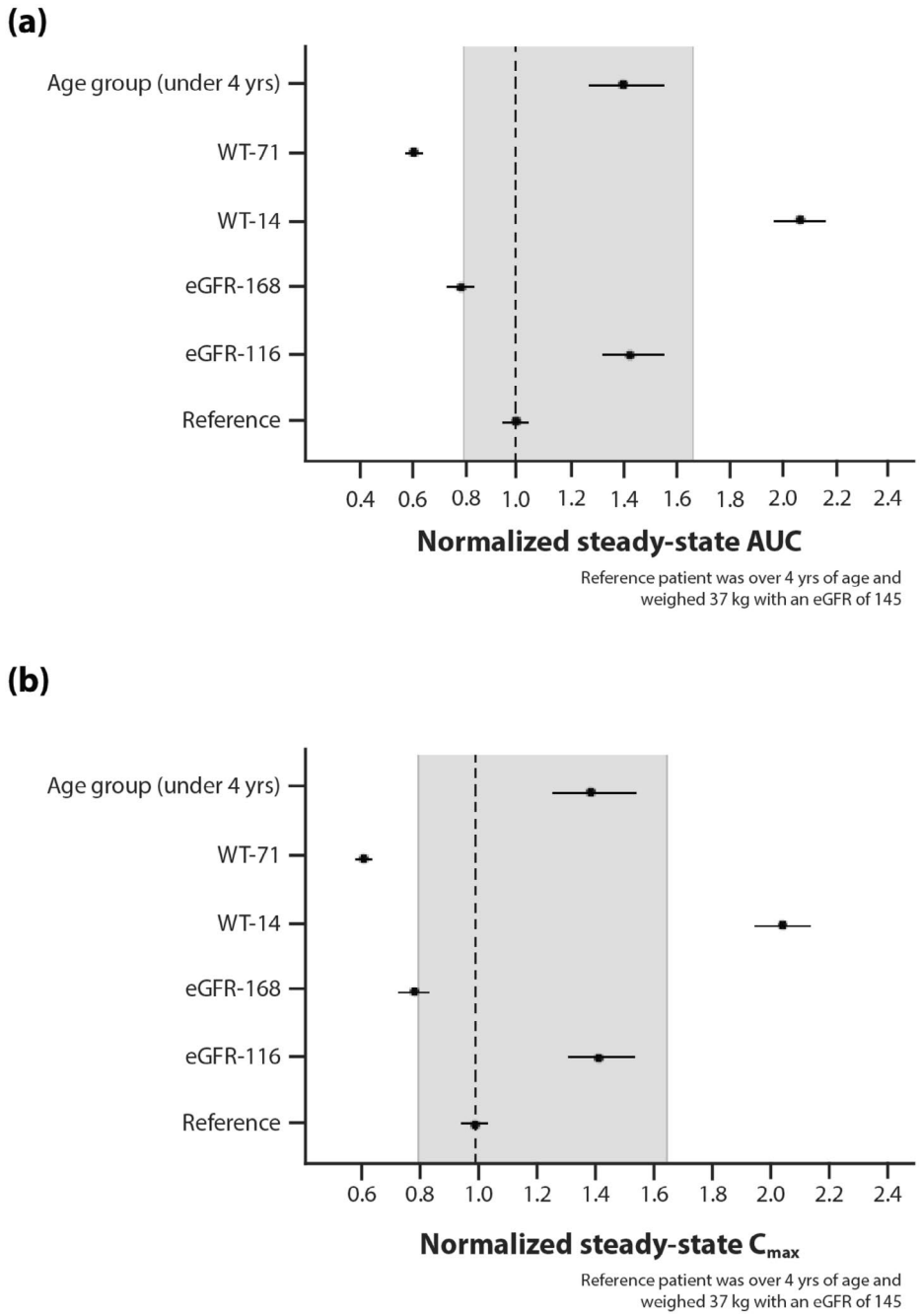

FIGURE 4 | Final PK model covariate effects on the normalized steady-state (a) AUC and (b) C_{max}. Gray shaded area represents the reference range of 0.8–1.67. eGFR (mL/min/1.73 m^2), WT (kg). AUC, area under the concentration–time curve; C_{max}, maximum concentration; eGFR, estimated glomerular filtration rate; PK, pharmacokinetic; WT, body weight.

4 | Discussion

This analysis represents the first integrated population PK model describing eteplirsen plasma PK in patients with DMD. The population PK data for eteplirsen were characterized by a three-compartment PK model with zero-order input and rapid first-order elimination across all dose levels. Model evaluations indicated that both the central tendency and the interindividual

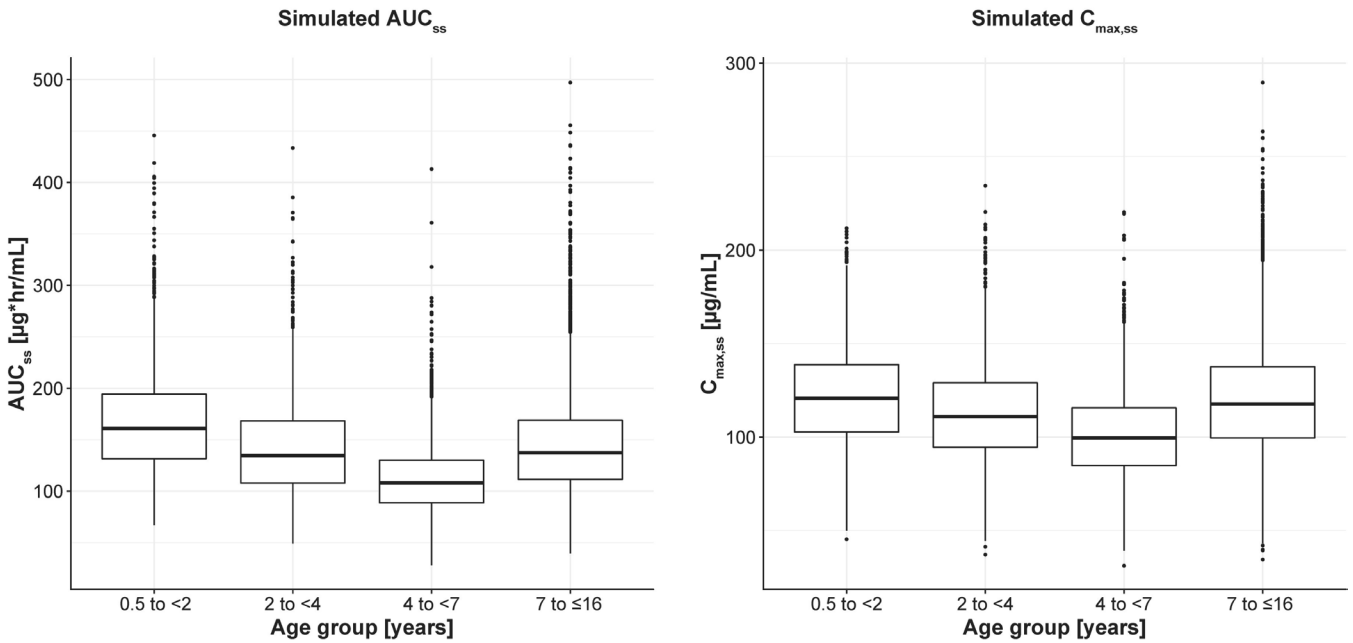

FIGURE 5 | Stochastic simulation using the final population PK model by age group. Boxes depict the 25th, 50th, and 75th percentiles of the data. Vertical lines extending from the boxes show the 25th percentile—1.5 × IQR and the 75th percentile + 1.5 × IQR, where IQR is the distance between the 25th and 75th percentiles. Outliers are marked outside of the vertical whisker lines by black circles. AUC_{ss}, area under concentration–time curve at steady state; $C_{max,ss}$, maximum concentration at steady state; IQR, interquartile range; PK, pharmacokinetic.

variability in the PK data across all doses and studies were generally well represented by the final model.

The population PK model demonstrated that plasma PK of eteplirsen was linear across a wide range of doses, suggesting a dose-proportional increase in exposure. Data from younger and older patients with DMD amenable to exon 51 skipping ($N = 157$) were integrated to characterize PK across a broad age range and moderate interindividual variation in eteplirsen exposure was observed in this population. The simulations showed similar exposures for eteplirsen 30 mg/kg IV once weekly across different age groups, with overlapping 95% CIs for both C_{max} and AUC, and exposures were within the variability expected for eteplirsen [29, 33]. These results are aligned with those derived from prior clinical trials where consistent PK characteristics of eteplirsen were shown using serial sampling in patients aged 5–15 years and sparse sampling in patients 6–48 months, supporting the existing eteplirsen dosing paradigm of uniform weight-based dosing across the broad target age range for DMD (6 months to 16 years old) [29, 33].

The model captured the effects of factors related to body growth (body weight and eGFR) in pediatric patients. As expected, body weight was an important predictor of plasma PK, supporting the current product label recommendation of weight-based dosing (30 mg/kg) [21]. eGFR was found to be an important covariate impacting eteplirsen exposure but did not reach statistical significance in this model. Because there was no subject with eGFR lower than 85.5 mL/min/1.73 m^2, it is unlikely that changes in the renal function would be noticeable and clinically significant. Furthermore, eGFR is normalized to body surface area, and given that body weight was included in the CL analysis using allometry, it is possible that eGFR does not have a significant effect considering the co-linearity between body surface area and body weight. However, it was important to include eGFR in the model considering the renal route of drug elimination and renal function maturation in these younger patients (6 months to 1 year), but model application below observed eGFR range would be limited.

DMD patients develop progressive muscle atrophy, with replacement of muscle mass with fat and fibrous tissue [42]. Muscle mass accounts for approximately 42% of the total body mass in healthy male subjects aged 18–29 years [43]. The median body weight in DMD patients is comparable with healthy subjects ranging in age from 2 to 12 years, but 90th percentile of body weight was significantly higher in DMD patients compared with healthy subjects. Both progressive muscle mass loss and wider distribution of body weight in DMD patients could have substantial impact on the PK of the drug that shows high muscle distribution.

A nonclinical study performed in mice using ^{14}C-eteplirsen showed that eteplirsen distributes in different tissues, including muscle and fat tissue (data on file, Sarepta Therapeutics Inc.). Therefore, muscle mass replacement with fat tissue would have limited impact on the eteplirsen plasma PK. As such, the final model included body weight effect using allometric scaling on PK parameters, and no additional adjustment for muscle mass loss in DMD patients was considered.

Applications of this population PK model could include projecting the clinical plasma PK profiles of eteplirsen following alternative dosing regimens. Additionally, considering that similar PK characteristics have been observed for eteplirsen and the PMOs golodirsen (exon 53 skipping) [27] and casimersen (exon 45 skipping) [28] in the preclinical setting [44], this work provides a rationale for weight-based dosing of other PMOs.

5 | Conclusion

Population PK modeling and simulations demonstrated consistent plasma exposure for the weight-based dosing regimen of eteplirsen 30 mg/kg/week across the broad age range of the target DMD population (6 months to adolescence). These results support the extrapolation of the 30 mg/kg weekly dosing regimen to younger patients (6 months to < 7 years) to achieve plasma exposures that are associated with observed efficacy in the older age groups (≥ 7 years to adolescence). Uniform weight-based dosing for eteplirsen is thus appropriate across a wide age range in patients with DMD.

Author Contributions

Y.P., L.O., N.Y., L.R.R.-K., and L.E. wrote the manuscript. L.E. designed the research. N.Y. performed the research. Y.P., L.O., L.R.R.-K., and L.E. analyzed the data.

Acknowledgments

The authors thank Claire Mukashyaka for contribution and support for the abstract presented at ACoP. Medical writing and editorial support were provided by Paraskevi Briassouli, PhD, and Matthew Bidgood, PhD, of Eloquent Scientific Solutions and were funded by Sarepta Therapeutics Inc.

Conflicts of Interest

All authors were employee of Sarepta Therapeutics Inc. at the time of data analysis, and may own stock/options in the company.

References

1. A. E. Emery, "Population Frequencies of Inherited Neuromuscular Diseases—A World Survey," *Neuromuscular Disorders* 1, no. 1 (1991): 19–29.

2. S. J. Moat, D. M. Bradley, R. Salmon, A. Clarke, and L. Hartley, "Newborn Bloodspot Screening for Duchenne Muscular Dystrophy: 21 Years Experience in Wales (UK)," *European Journal of Human Genetics* 21, no. 10 (2013): 1049–1053.

3. P. A. Romitti, Y. Zhu, S. Puzhankara, et al., "Prevalence of Duchenne and Becker Muscular Dystrophies in the United States," *Pediatrics* 135, no. 3 (2015): 513–521.

4. S. Ryder, R. M. Leadley, N. Armstrong, et al., "The Burden, Epidemiology, Costs and Treatment for Duchenne Muscular Dystrophy: An Evidence Review," *Orphanet Journal of Rare Diseases* 12, no. 1 (2017): 79.

5. S. Crisafulli, J. Sultana, A. Fontana, F. Salvo, S. Messina, and G. Trifirò, "Global Epidemiology of Duchenne Muscular Dystrophy: An Updated Systematic Review and Meta-Analysis," *Orphanet Journal of Rare Diseases* 15, no. 1 (2020): 141.

6. D. J. Birnkrant, K. Bushby, C. M. Bann, et al., "Diagnosis and Management of Duchenne Muscular Dystrophy, Part 1: Diagnosis, and Neuromuscular, Rehabilitation, Endocrine, and Gastrointestinal and Nutritional Management," *Lancet Neurology* 17, no. 3 (2018): 251–267.

7. D. Duan, N. Goemans, S. Takeda, E. Mercuri, and A. Aartsma-Rus, "Duchenne Muscular Dystrophy," *Nature Reviews. Disease Primers* 7, no. 1 (2021): 13.

8. N. Elangkovan and G. Dickson, "Gene Therapy for Duchenne Muscular Dystrophy," *Journal of Neuromuscular Diseases* 8, no. s2 (2021): S303–S316.

9. C. M. McDonald, E. K. Henricson, J. J. Han, et al., "The 6-Minute Walk Test in Duchenne/Becker Muscular Dystrophy: Longitudinal Observations," *Muscle & Nerve* 42, no. 6 (2010): 966–974.

10. E. S. Mazzone, M. Pane, M. P. Sormani, et al., "24 Month Longitudinal Data in Ambulant Boys With Duchenne Muscular Dystrophy," *PLoS One* 8, no. 1 (2013): e52512.

11. E. Henricson, R. Abresch, J. J. Han, et al., "Percent-Predicted 6-Minute Walk Distance in Duchenne Muscular Dystrophy to Account for Maturational Influences," *PLoS Currents* 4 (2012): RRN1297.

12. V. Ricotti, D. A. Ridout, M. Pane, et al., "The NorthStar Ambulatory Assessment in Duchenne Muscular Dystrophy: Considerations for the Design of Clinical Trials," *Journal of Neurology, Neurosurgery, and Psychiatry* 87, no. 2 (2016): 149–155.

13. E. Mercuri, C. G. Bonnemann, and F. Muntoni, "Muscular Dystrophies," *Lancet* 394, no. 10213 (2019): 2025–2038.

14. J. M. Kwon, H. Z. Abdel-Hamid, S. A. Al-Zaidy, et al., "Clinical Follow-Up for Duchenne Muscular Dystrophy Newborn Screening: A Proposal," *Muscle & Nerve* 54, no. 2 (2016): 186–191.

15. P. Beckers, J. H. Caberg, V. Dideberg, et al., "Newborn Screening of Duchenne Muscular Dystrophy Specifically Targeting Deletions Amenable to Exon-Skipping Therapy," *Scientific Reports* 11, no. 1 (2021): 3011.

16. Q. Ke, Z. Y. Zhao, J. R. Mendell, et al., "Progress in Treatment and Newborn Screening for Duchenne Muscular Dystrophy and Spinal Muscular Atrophy," *World Journal of Pediatrics* 15, no. 3 (2019): 219–225.

17. L. J. Popplewell, C. Trollet, G. Dickson, and I. R. Graham, "Design of Phosphorodiamidate Morpholino Oligomers (PMOs) for the Induction of Exon Skipping of the Human DMD Gene," *Molecular Therapy* 17, no. 3 (2009): 554–561.

18. J. R. Mendell, L. R. Rodino-Klapac, Z. Sahenk, et al., "Eteplirsen for the Treatment of Duchenne Muscular Dystrophy," *Annals of Neurology* 74, no. 5 (2013): 637–647.

19. A. Aartsma-Rus, I. Fokkema, J. Verschuuren, et al., "Theoretic Applicability of Antisense-Mediated Exon Skipping for Duchenne Muscular Dystrophy Mutations," *Human Mutation* 30, no. 3 (2009): 293–299.

20. S. D. Wilton, A. M. Fall, P. L. Harding, G. McClorey, C. Coleman, and S. Fletcher, "Antisense Oligonucleotide-Induced Exon Skipping Across the Human Dystrophin Gene Transcript," *Molecular Therapy* 15, no. 7 (2007): 1288–1296.

21. "Exondys 51 (Eteplirsen) Injection, for Intravenous Use [Package Insert]," (2022), accessed December 9, 2024, https://www.accessdata.fda.gov/drugsatfda_docs/label/2022/206488s027s028s029lbl.pdf.

22. P. Sazani, K. P. Ness, D. L. Weller, et al., "Chemical and Mechanistic Toxicology Evaluation of Exon Skipping Phosphorodiamidate Morpholino Oligomers in mdx Mice," *International Journal of Toxicology* 30, no. 3 (2011): 322–333.

23. P. Sazani, K. P. Ness, D. L. Weller, et al., "Repeat-Dose Toxicology Evaluation in Cynomolgus Monkeys of AVI-4658, a Phosphorodiamidate Morpholino Oligomer (PMO) Drug for the Treatment of Duchenne Muscular Dystrophy," *International Journal of Toxicology* 30, no. 3 (2011): 313–321.

24. P. Sazani, D. L. Weller, and S. B. Shrewsbury, "Safety Pharmacology and Genotoxicity Evaluation of AVI-4658," *International Journal of Toxicology* 29, no. 2 (2010): 143–156.

25. M. P. Carver, J. S. Charleston, C. Shanks, et al., "Toxicological Characterization of Exon Skipping Phosphorodiamidate Morpholino Oligomers (PMOs) in Non-human Primates," *Journal of Neuromuscular Diseases* 3, no. 3 (2016): 381–393.

26. P. R. Clemens, V. K. Rao, A. M. Connolly, et al., "Safety, Tolerability, and Efficacy of Viltolarsen in Boys With Duchenne Muscular Dystrophy Amenable to Exon 53 Skipping: A Phase 2 Randomized Clinical Trial," *JAMA Neurology* 77, no. 8 (2020): 982–991.

27. D. E. Frank, F. J. Schnell, C. Akana, et al., "Increased Dystrophin Production With Golodirsen in Patients With Duchenne Muscular Dystrophy," *Neurology* 94, no. 21 (2020): e2270–e2282.

28. K. R. Wagner, N. L. Kuntz, E. Koenig, et al., "Safety, Tolerability, and Pharmacokinetics of Casimersen in Patients With Duchenne Muscular Dystrophy Amenable to Exon 45 Skipping: A Randomized, Double-Blind, Placebo-Controlled, Dose-Titration Trial," *Muscle & Nerve* 64, no. 3 (2021): 285–292.

29. E. Mercuri, A. M. Seferian, L. Servais, et al., "Safety, Tolerability and Pharmacokinetics of Eteplirsen in Young Boys Aged 6-48 Months With Duchenne Muscular Dystrophy Amenable to Exon 51 Skipping," *Neuromuscular Disorders* 33, no. 6 (2023): 476–483.

30. C. M. McDonald, P. B. Shieh, H. Z. Abdel-Hamid, et al., "Open-Label Evaluation of Eteplirsen in Patients With Duchenne Muscular Dystrophy Amenable to Exon 51 Skipping: PROMOVI Trial," *Journal of Neuromuscular Diseases* 8, no. 6 (2021): 989–1001.

31. J. R. Mendell, N. Goemans, L. P. Lowes, et al., "Longitudinal Effect of Eteplirsen Versus Historical Control on Ambulation in Duchenne Muscular Dystrophy," *Annals of Neurology* 79, no. 2 (2016): 257–271.

32. J. R. Mendell, N. Khan, N. Sha, et al., "Comparison of Long-Term Ambulatory Function in Patients With Duchenne Muscular Dystrophy Treated With Eteplirsen and Matched Natural History Controls," *Journal of Neuromuscular Diseases* 8, no. 4 (2021): 469–479.

33. S. Cirak, V. Arechavala-Gomeza, M. Guglieri, et al., "Exon Skipping and Dystrophin Restoration in Patients With Duchenne Muscular Dystrophy After Systemic Phosphorodiamidate Morpholino Oligomer Treatment: An Open-Label, Phase 2, Dose-Escalation Study," *Lancet* 378, no. 9791 (2011): 595–605.

34. National Library of Medicine, "ClinicalTrials.gov. Safety Study of Eteplirsen to Treat Early Stage Duchenne Muscular Dystrophy: Results Overview (NCT02420379)," accessed December 9, 2024, https://clinicaltrials.gov/study/NCT02420379?term=NCT02420379&rank=1&tab=results.

35. A. S. Levey, L. A. Stevens, C. H. Schmid, et al., "A New Equation to Estimate Glomerular Filtration Rate," *Annals of Internal Medicine* 150, no. 9 (2009): 604–612.

36. L. Viollet, S. Gailey, D. J. Thornton, et al., "Utility of Cystatin C to Monitor Renal Function in Duchenne Muscular Dystrophy," *Muscle & Nerve* 40, no. 3 (2009): 438–442.

37. C. R. Villa, A. Kaddourah, J. Mathew, et al., "Identifying Evidence of Cardio-Renal Syndrome in Patients With Duchenne Muscular Dystrophy Using Cystatin C," *Neuromuscular Disorders* 26, no. 10 (2016): 637–642.

38. A. Aldenbratt, C. Lindberg, E. Johannesson, O. Hammarsten, and M. K. Svensson, "Estimation of Kidney Function in Patients With Primary Neuromuscular Diseases: Is Serum Cystatin C a Better Marker of Kidney Function Than Creatinine?," *Journal of Nephrology* 35, no. 2 (2022): 493–503.

39. I. Mahmood, "Dosing in Children: A Critical Review of the Pharmacokinetic Allometric Scaling and Modelling Approaches in Paediatric Drug Development and Clinical Settings," *Clinical Pharmacokinetics* 53, no. 4 (2014): 327–346.

40. Centers for Disease Control and Prevention, "National Health and Nutrition Examination Survey," accessed December 9, 2024, https://www.cdc.gov/nchs/nhanes/.

41. N. A. West, M. L. Yang, D. A. Weitzenkamp, et al., "Patterns of Growth in Ambulatory Males With Duchenne Muscular Dystrophy," *Journal of Pediatrics* 163, no. 6 (2013): 1759–1763.e1751.

42. S. S. Summer, B. L. Wong, M. M. Rutter, et al., "Age-Related Changes in Appendicular Lean Mass in Males With Duchenne Muscular Dystrophy: A Retrospective Review," *Muscle & Nerve* 63, no. 2 (2021): 231–238.

43. I. Janssen, S. B. Heymsfield, Z. Wang, and R. Ross, "Skeletal Muscle Mass and Distribution in 468 Men and Women Aged 18–88 Yr," *Journal of Applied Physiology* 89, no. 1 (2000): 81–88.

44. M. C. Mukashyaka, Y. Patel, P. Burch, B. Hunter, L. R. Rodino-Klapac, and L. East, "Characterization of Nonclinical Drug Metabolism and Pharmacokinetic Properties Shows Consistency Among Three Phosphorodiamidate Morpholino Oligonucleotides FDA-Approved for Duchenne Muscular Dystrophy," in *Presented at the 13th International Meeting of the International Society for the Study of Xenobiotics, September 11–14, 2022, Seattle, Washington, USA*.

Supporting Information

Additional supporting information can be found online in the Supporting Information section.